THE JOURNAL OF PHYSICAL CHEMISTRY B

Article

pubs.acs.org/JPCB

Two-Dimensional Infrared Spectroscopy of Isotope-Diluted Low Density Amorphous Ice

Andrey Shalit, Fivos Perakis, and Peter Hamm*

Department of Chemistry, University of Zurich, Winterthurerstrasse 190, CH-8057 Zurich, Switzerland

ABSTRACT: We present two-dimensional (2D) infrared (IR) spectra of isotope diluted ice in its low density amorphous form. Amorphous ice, which is structurally more similar to liquid water than to crystalline ice, provides higher resolution spectra of the hydrogen bond potentials because all motion is frozen. In the case of OD vibration of HOD in H_2O, diagonal and off-diagonal (intermode) anharmonicity as well as the relaxation rate of the first excited state increase with hydrogen bond strength in a consistent way. For the OH vibration of HOD in D_2O, additional more specific couplings need to be taken into account to explain the 2D IR response, that is, a Fermi resonance with the HOD bend vibration and couplings to phonon modes that lead to quantum beating. The lifetime of the fist excited state, 240 fs, is the shortest ever reported for any phase of isotope diluted water.

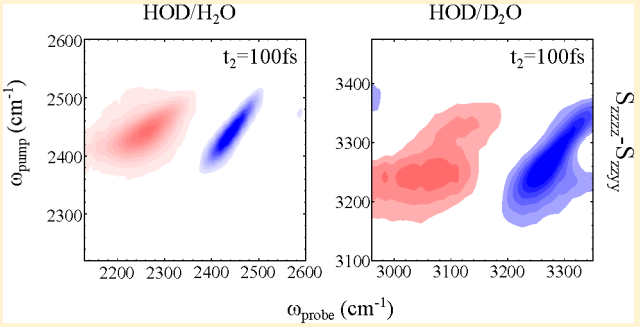

I. INTRODUCTION

Among the various forms of ice (at least 15 different crystalline phases are known[1,2]), the amorphous state is of particular interest as it possess properties of both an unordered liquid and an ordered solid state. Three different forms of amorphous ice exist which are distinguished by their densities: low density (LDA), high density (HDA), and very high density (vHDA).[3,4] Amorphous ice found its relevance in a wide range of research areas from biology, where it is used for electron cryomicroscopy,[5] to astrophysics, as most of the ice in the universe is assumed to be amorphous.[6] The structure of amorphous ice is a crucial aspect in a comprehensive understanding of the thermodynamic properties of water;[7] in particular in light of the liquid-to-liquid phase transition hypothesis put forward by Stanley and co-workers to account for the anomalous thermodynamic properties of water.[8,9] That is, two distinct liquid phases in the deeply supercooled regime are predicted (low-density liquid LDL and high-density liquid HDL), which are believed to be associated with the corresponding amorphous ice phases, LDA and HDA, respectively.[10−13]

Various spectroscopic techniques have been applied to characterize amorphous ice, including Fourier transform infrared (FTIR) spectroscopy,[14,15] Raman spectroscopy,[16,17] X-ray diffraction,[18,19] and neutron diffraction.[20,21] As expected, the radial distribution function from diffraction experiments confirms the absence of the long-range periodic structure in the amorphous ices.[4,22] This observation underlines the closer resemblance of amorphus ice to liquid water rather than to other crystalline phases of ice, although substantial differences in the local structure of LDA and HDA have been reported.[21]

While crystalline ice Ih has been studied extensively also by nonlinear vibrational spectroscopic tools,[23−27] to the best of our knowledge, no such measurements have ever been performed for amorphous ice. Nonlinear vibrational spectroscopy, such as two-dimensional infrared spectroscopy (2D IR),[26−33] is an excellent tool to monitor the local structure and dynamic properties of the hydrogen bonds in water. These experiments make use of the fact that the vibrational frequency of the OH stretch vibration is highly correlated with the OO distance of a pair of hydrogen bonded water molecules.[34−38] That is, a shorter and therefore stronger hydrogen bond results in a larger red shift of the OH stretch vibration. Due to its disorder, amorphous ice preserves a wide frequency distribution for the OH stretch vibration—similar to liquid water but considerably less than in crystalline forms of ice—allowing one to investigate a wide range of hydrogen bond environments. On the other hand, the sample remains frozen on the time scale of an IR experiment, thus reorientational dynamics and spectral diffusion will not affect the spectroscopic response.

In this paper, we present 2D IR spectra of the OD and the OH stretch vibration of HOD in H_2O and D_2O, respectively, in LDA ice. For the OD vibration of HOD in H_2O, we show that a single mode picture can describe the 2D IR response well, with an anharmonicity and relaxation rate that both increase with hydrogen bond strength. For the OH vibration of HOD in D_2O, the situation is more complicated and specific couplings to other modes, such as a Fermi resonance with the HOD bend vibration or coupling to phonon modes, need to be taken into account to explain the 2D IR response.

Special Issue: Michael D. Fayer Festschrift

Received: May 31, 2013
Revised: July 23, 2013
Published: August 2, 2013

II. EXPERIMENTAL METHODS

A commercial Ti:sapphire oscillator with chirped pulse amplifier was used to seed a home-built optical parametric amplifier (OPA)[39] to produce tunable mid-IR pulses with 250 cm^{-1} bandwidth. Central frequencies of 2450 and 3300 cm^{-1} were used for the OD and OH stretch vibration, respectively. 2D IR spectra were recorded using a Fourier transform setup in pump−probe geometry,[40] where the data acquisition is performed with a fast scanning routine, described in detail elsewhere.[41] In brief, the mid-IR beam is split into a pump pulse and a probe pulse. The pump pulse travels through an interferometer, generating a phase-locked pair of pulses, where time delay between the two arms is referred to as coherence time t_1. Subsequently, a second delay stage shifts the two pump pulses with respect to the probe pulse, referred to as population time t_2. We scanned t_1 = (−300, 1000) fs and recorded spectra for various t_2 delays up to 3 ps. A wobbling Brewster window was used for scattering suppression.[42] The polarization of the two pump pulses relative to that of the probe pulse was controlled with the help of a $\lambda/2$-plate, and both S_{ZZZZ} and S_{ZZYY} spectra were measured to calculate the anisotropic ($S_{ZZZZ} - S_{ZZYY}$) and isotropic ($S_{ZZZZ} + 2S_{ZZYY}$)/3 spectra.

Isotope-diluted LDA ice samples were prepared by slowly depositing water vapor (2.5% of D_2O in H_2O or 2.5% H_2O in H_2O, respectively) onto a cold CaF_2 window held at 80 K inside an evacuated, nitrogen-cooled flow cryostat.[43,44] The water has been degassed before deposition by a freeze−pump−thaw procedure. The creation of LDA ice requires a deposition rate of at most 2 μm/min;[44] our average deposition rate was much lower with of 0.1 μm/min. Absorption spectra were monitored in situ during the deposition and compared to literature data[14] to ensure that the ice layer was indeed amorphous. The deposition process was stopped when an optical density of 0.4 was reached.

III. RESULTS

A. IR Absorption Spectra. Figure 1 shows normalized IR absorption spectra of LDA ice prepared according to the procedure described above (green solid line), of crystalline ice Ih prepared by cooling a thin film of liquid water down to 80 K (red dotted line) and of room-temperature liquid water (blue dashed line). The sample is isotope-diluted water with 5% HOD in either H_2O (Figure 1a) or D_2O (Figure 1b), and we look at an isolated OD or OH stretch vibration of HOD, respectively. The observed lineshapes are in good agreement with those obtained by Rice et al.[14] under similar conditions. In both cases, LDA ice and liquid water exhibit a relatively broad and featureless absorption band due to the disorder in the sample. The peak is more red-shifted in LDA ice, as compared to liquid water, indicating in average stronger hydrogen bonds. That trend is already observed in liquid water, for which a colder sample exhibits a more red-shifted absorption frequency.[45] Nevertheless, the red-shift of the peak in LDA ice remains less than that of crystalline ice Ih, since in the latter case, all waters are involved in a perfectly tetrahedral hydrogen bond environment.

B. 2D IR Spectra of the OD Stretch Vibration of HOD/H_2O. A selection of normalized 2D IR spectra of the OD stretch vibration of HOD/H_2O in LDA ice at 80 K is shown in Figure 2 for population times t_2 of 100 fs, 500 fs, 1 ps, and 3 ps. The on-diagonal peak depicted in blue (label I) is associated with bleach and stimulated emission between the ground state

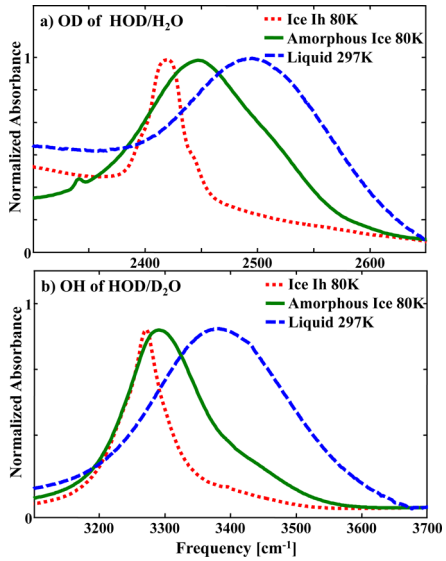

Figure 1. Normalized absorption spectrum of LDA ice at 80 K (green solid line), ice Ih at 80 K (red dotted line), and liquid room-temperature water (blue dashed line). (a) OD stretch mode of HOD in H_2O. (b) OH stretch mode of HOD in D_2O. The small peak at 2340 cm^{-1} in part a originates from trace amounts of CO_2 in LDA.

and the first excited state (0−1 transition), while the oppositely signed red peak (label II) is due to the anharmonically shifted excited state absorption from the first to the second excited state (1−2 transition). The upper row of Figure 2 shows the evolution of the anisotropic signal ($S_{ZZZZ} - S_{ZZYY}$) and lower row that of the isotropic signal ($S_{ZZZZ} + 2S_{ZZYY}$)/3. The polarization dependence allows us to distinguish an orientation dependent (anisotropic) contribution from any orientation independent contributions (isotropic). In the glassy state of LDA ice, orientational relaxation of the water molecules is expected to be completely absent, so the excited molecules maintain the anisotropy induced by the pump−pulse polarization. However, once the excited state of these molecules decays, the environment will be heated up, which affects many water molecules in the vicinity with various orientations, so any signal originating from heating will essentially be isotropic. Therefore, measuring the anisotropic signal $S_{ZZZZ} - S_{ZZYY}$ is an efficient way to suppress heating effects and to be selective to the relaxation dynamic of the initially excited water molecules.

In the anisotropic spectra (Figure 2, top row), the 0−1 peak is strongly elongated along the diagonal, reflecting a pronounced inhomogenous broadening of the OD stretch frequency,[33] as expected for a glassy environment.[46] The slope of the 0−1 peak is 45°, because the pump and probe frequencies are perfectly correlated. The 0−1 peak hardly changes shape as a function of population time, because there is essentially no spectral diffusion on the time scale of the experiment and the inhomogeneous broadening is static; again, as expected for a glassy state.

The 1−2 excited state absorption peak is different in shape. First, the tilt of the peak is larger, as highlighted by the black lines in the 500 fs spectrum of Figure 2, top. These lines were generated by connecting the maxima (for the 1−2 transition) or minima (for 0−1 transition) of spectral slices along the ω_{pump} axis.[47] The separation of the 0−1 peak from the 1−2 peak along the probe-frequency axis reflects the diagonal anharmonicity of the OD potential. Given the different tilt angles of both peaks, the amount of diagonal anharmonicity

dx.doi.org/10.1021/jp4053743 | J. Phys. Chem. B 2013, 117, 15512−15518

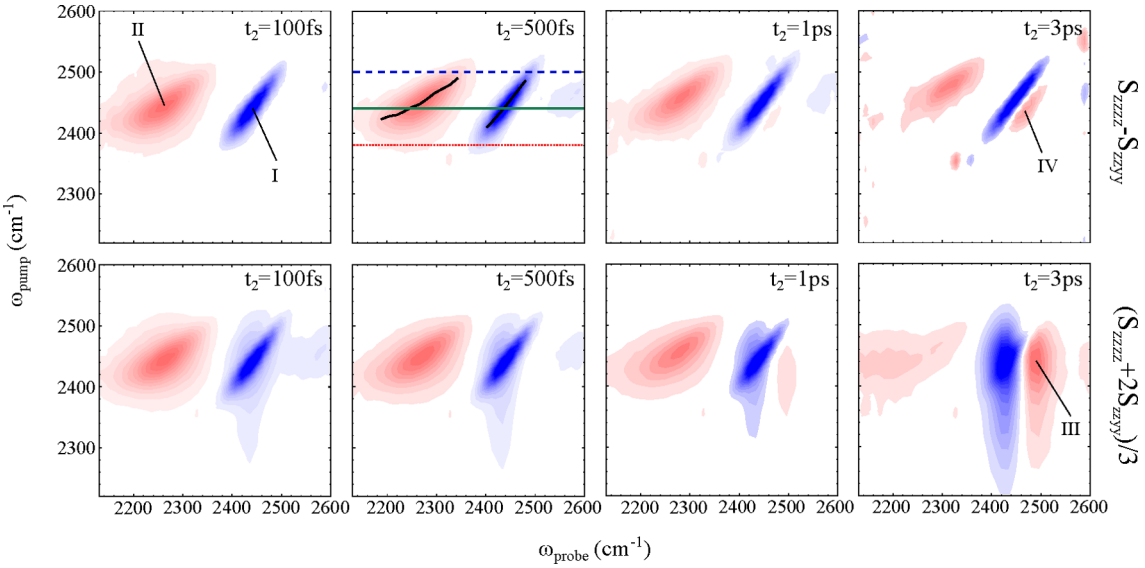

Figure 2. Series of normalized 2D IR spectra of the OD stretch vibration of LDA ice with 5% HOD in H_2O at 80 K for population times t_2 of 100 fs, 500 fs, 1 ps, and 3 ps. By convention, we depict the pump frequency axis (ω_{pump}) vertically and the probe frequency axis (ω_{probe}) horizontally. (upper row) Anisotropic spectra ($S_{ZZZZ} - S_{ZZYY}$). (lower row) Isotropic spectra ($S_{ZZZZ} + 2S_{ZZYY}$)/3. The black lines in the anisotropic 500 fs spectrum depicts the peak of the signal, and the colored horizontal lines the frequency positions for which the cuts in Figure 3 are taken. Labels I–IV indicate features discussed in the text.

varies with hydrogen bond strength. Second, the 1–2 peak is broader than the 0–1 peak, and its width varies with frequency as well. This effect is better seen in the cuts shown in Figure 3. The 1–2 peak becomes broader as the pump frequency is decreased from 2500 cm^{-1} (dashed blue line) through 2440 cm^{-1} (solid green line) down to 2380 cm^{-1} (dotted red line).

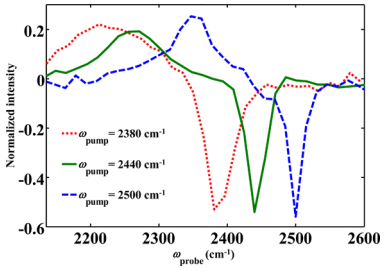

Figure 3. Normalized slices of the 2D IR spectrum at t_2 = 500 fs and at the pump frequencies indicated in Figure 2, i.e., along ω_{pump} = 2380 (red dotted line), 2440 (green solid line), and 2500 cm^{-1} (blue dashed line).

Also the vibrational relaxation rate has a pronounced frequency dependence. Figure 4 presents the relaxation dynamics of the OD stretch vibration of HOD in H_2O extracted from the anisotropic 2D spectra for various pump frequencies (the decay is not seen in Figure 2 because these spectra are normalized). The upper panel depicts the decay of the 1–2 signal, the lower that of the corresponding 0–1 signal. All data were fitted with a single exponential decay function (dashed lines in Figure 4). The time constants deduced from the 1–2 and the 0–1 signals are roughly the same within experimental error (the small difference is discussed below), and the decay time constants increase with pump frequency from ≈500 fs (i.e., 550 and 430 fs for 0–1 and 1–2 transitions, respectively) on the red side of the band to ≈1.2 ps on the blue side (see Table I).

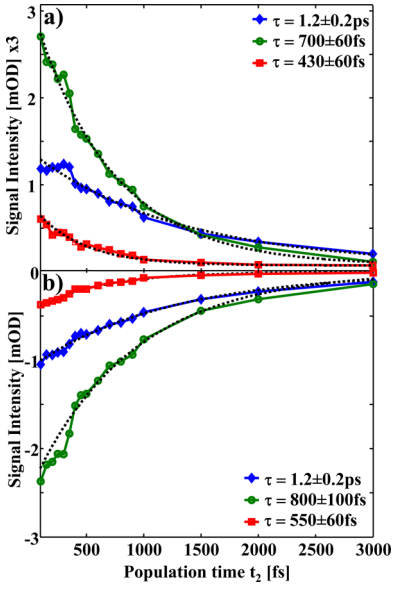

Figure 4. Relaxation dynamics of (a) the maximum of the 1–2 transition and (b) the minimum of the 0–1 transitions of the OD stretch for three transient signals depicted in Figure 3 with consistent color code.

Table I. Decay Time Constants of the OD Stretch Vibration in HOD/H_2O (Figure 4) and the OH Stretch Vibration in HOD/D_2O (Figure 6) at the Pump Frequencies Indicated[a]

	OD			OH
	2380 cm^{-1}	2440 cm^{-1}	2500 cm^{-1}	3280 cm^{-1}
0–1	550 ± 60 fs	800 ± 100 fs	1.2 ± 0.2 ps	580 ± 70 fs
1–2	430 ± 60 fs	700 ± 60 fs	1.2 ± 0.2 ps	240 ± 80 fs

[a]Time constants are deduced for both the 0–1 and the 1–2 signals.

The isotropic signal depicted in the lower panel of Figure 2 shows how the thermal contributions influences the shape of

dx.doi.org/10.1021/jp4053743 | J. Phys. Chem. B 2013, 117, 15512–15518

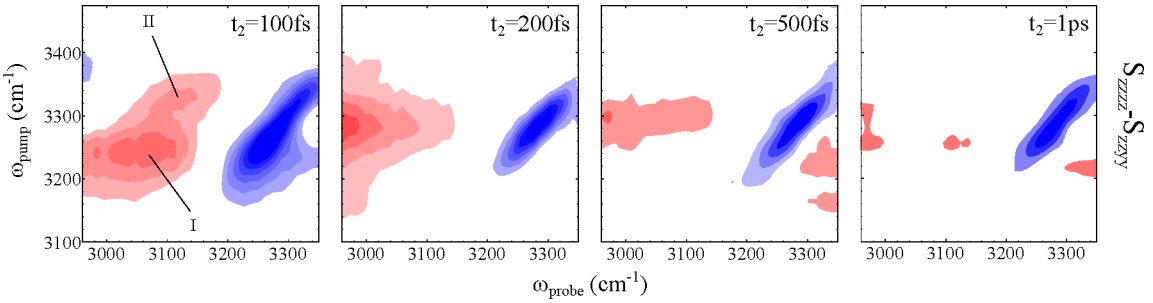

Figure 5. Series of anisotropic ($S_{ZZZZ} - S_{ZZYY}$) normalized 2D IR spectra of the OH stretch vibration of LDA ice with 5% HOD in D_2O at 80 K for population times t_2 of 100 fs, 200 fs, 500 fs, and 1 ps.

the 0−1 peak at later population times. As the population time increases, its line shape becomes more vertical and an additional blue-shifted signal appears (label III). This signal originates from the overall weaker hydrogen bonds of surrounding HOD molecules, whose intermolecular degrees of freedom have been heated by the energy dissipated after relaxation of the initially excited HOD molecule.[24] In addition, the bleach of these HOD molecules superimposes with the 0−1 band of the initially excited water molecules and thus also affects the line shape of the 0−1 band. The heat signal originates from HOD molecules that sit in different hydrogen bond environments, i.e. with different OD stretch frequencies, hence the thermal contribution is hardly correlated with the frequency of the initially excited water molecule and their line shape is vertical. It is interesting to note that an additional blue-shifted contribution is also visible in the anisotropic response at late population times (3 ps, label IV). Its line shape is however tilted, because it originates from heating of intermolecular degrees of freedom of the initially excited water molecules; hence, pump and probe frequency are correlated. In principle, this heat signal should show up before heat diffuses to other HOD molecules in the vicinity, which are the ones giving rise to an isotropic signal, but due to the high concentration of HOD (5%), we were not able to distill out that propagation effect.

As a side remark, it is important not to misinterpret the gradual change of the isotropic 0−1 line shape from tilted to vertical as spectral diffusion. Spectral diffusion is a main mechanism for such line shape changes in liquid water[28−32]), but the glassy state assures that there is no rearrangement of hydrogen bonds on the time scale of the experiment.

C. 2D IR Spectra of the OH Stretch Vibration of HOD/D_2O. A complementary set of anisotropic 2D IR spectra of the OH stretch vibration of 5% HOD in D_2O is shown in Figure 5 for population times of 100 fs, 200 fs, 500 fs, and 1 ps (similarly to the OD case, the isotropic 2D IR spectra contain a thermal contribution at longer population times, but do not add any new aspect and hence are not discussed here). The line shape of the 0−1 band is elongated along the diagonal and hardly changes in shape as a function of population time, similar to what has been observed for the OD stretch vibration (Figure 2). The peak of 0−1 transition of the OH stretch vibration observed in the 2D experiments is slightly blue-shifted with respect to the linear absorption spectrum (the same effect is visible also for the OD stretch vibration, albeit to a much smaller extent). This shift is probably due to the non-Condon effects discussed by Skinner and co-workers.[48] The transition dipole moment of the OH stretch vibration is higher for stronger hydrogen bond environments, i.e. for lower frequencies. As the 2D response scales with the fourth power of the transition dipole moment while the linear response scales only with the second power, this effect shifts the center-of-mass of the 2D response to lower frequencies.

The 1−2 peak of the OH stretch is quite different from that of the OD stretch. First, it exhibits a double peak structure (labels I and II in Figure 5), and second, the 1−2 peaks decays much quicker than the 0−1 peak, which is highlighted in Figure 6. An exponential fit reveals a 240 fs decay constant for the 1−2 peak, while the 0−1 peak decays within 580 fs (see Table I).

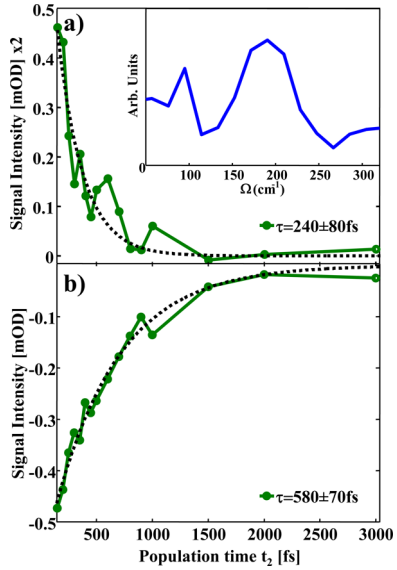

Figure 6. Relaxation dynamics of the 1−2 (a) and 0−1 (b) transitions at ω_{pump} = 3280 cm^{-1} of the OH stretch vibration of HOD in D_2O. The inset shows the Fourier transform (power spectrum) of the 1−2 signal.

In addition, a complex beating pattern is superimposed, which is more pronounced for the 1−2 transition (some beating is also observed for the OD stretch vibration in Figure 4, which is however not analyzed due to its smallness). The inset of Figure 6 shows a Fourier transform of the 1−2 data after subtraction of the exponential decay and interpolation of the data onto equidistant time steps for 50 fs. A pronounced peak is observed at ≈200 cm^{-1}, which coincides with the hydrogen bond stretch coordinate observed also in liquid water.[37,49,50] Interestingly, a somewhat lower frequency (i.e., 150 cm^{-1}) has been observed in ice Ih for presumably the same type of mode.[25,26] In addition, a lower frequency peak at ≈100 cm^{-1} is found whose assignment is presently unclear (to the

dx.doi.org/10.1021/jp4053743 | J. Phys. Chem. B 2013, 117, 15512−15518

best of our knowledge, no equivalent feature has been discussed for liquid water).

IV. DISCUSSION

Hydrogen bonds in LDA ice are on average stronger than those in liquid water, as deduced from a larger red shift of the absorption band (Figure 1), but the width of the distribution of hydrogen bond strengths as well as the amount of inhomogeneous broadening is comparable. The latter is deduced from the tilt of the 2D IR line shape, which reflects the correlation of pump and probe frequencies and which has been observed also for liquid water at early enough population times.[28−32] However, water molecules are highly mobile in liquid water and exchange hydrogen bond partners on a 1 ps time scale. Consequently, the correlation between pump and probe frequency, or in other words the tilt of the 2D IR line shape, decreases on that time scale; a process called spectral diffusion. The same is not expected, and also not observed, for LDA ice. In particular the 0−1 peak in the anisotropic data of the OD stretch vibration of HOD in H_2O (Figure 2, top row) is strongly elongated along the diagonal and does essentially not change in shape as a function of population time. Crystalline ice Ih is static as well, but in contrast to LDA ice, the 2D IR line shape hardly reveals any inhomogeneity since all hydrogen bonds are essentially equivalent.[26]

The complete lack of spectral diffusion in LDA ice allows one to investigate the spectroscopic properties of water molecules as a function of hydrogen bond strength, the latter of which stays constant during the measurement (in contrast to liquid water). We discuss the OD stretch vibration of HOD/H_2O first since its response is simpler. In that case, all three spectral features we presented, i.e., the diagonal anharmonicity, the width of the 1−2 band as well as the relaxation time, vary with hydrogen bond strength in a consistent way.

Hydrogen bonding softens the OD potential, resulting in the red-shift of the absorption band. But hydrogen bonding not only has an effect on the harmonic part of the potential (measured via the 0−1 transition frequency) but induced also additional anharmonicity. That is, the diagonal anharmonicity, i.e., the difference between 0−1 and 1−2 transition frequencies, increases with stronger hydrogen bonding, and so does the asymmetry in line width width of the 1−2 band versus that of the 0−1 band (Figure 3). The larger width of the 1−2 transition has been assigned in refs 26 and 51 to off-diagonal (intermode) anharmonic coupling to intermolecular O···O modes, which according to our results become stronger with increasing hydrogen bond strength.

An enhanced anharmonic coupling of the OD excited state to other degrees of freedom also increases its vibrational relaxation rate (Figure 4). It is also interesting to note that the relaxation rate correlates with hydrogen bond strength rather independently from the thermodynamic phase in which water is investigated. That is, in terms of its hydrogen bond strength, LDA ice bridges the regimes from ice Ih to the liquid phase (Figure 1). The decay rate at the lower frequency side of LDA ice at 2380 cm^{-1} (550 and 430 fs for 0−1 and 1−2 transitions, respectively) is very much comparable to that observed in ice Ih under similar conditions (410 and 360 fs for 0−1 and 1−2 transitions, respectively)[26] while the value we find at the high frequency side at 2500 cm^{-1} (1.2 ps) is close to that observed for liquid water (1.4 ps).[28]

The response of the OH stretch vibration of HOD/D_2O is more complicated. First, the 1−2 peak exhibits a double peak structure (labels I and II in Figure 5), which we tentatively attribute to a Fermi resonance between the first overtone of the OH stretch vibration and a combination mode that contains 1 quantum of OH stretch and 2 quanta of HOD bend, which happen to be almost perfectly resonant for the OH stretch vibration.[52] Furthermore, they tune differently as a function of hydrogen bond strength, and they might in fact cross in the frequency range of interest (see Figure 2 of ref 52), thus explaining the double peak structure. However, we cannot exclude possible modulations of the signal due to the pulse overlap at early population times also being responsible for the complicated line shape.

Second, the decay of the 1−2 peak is significantly faster (240 fs) than that of the 0−1 peak. The 1−2 peak corresponds to the absorption from the first to the second excited state, and as such, its decay reports on the lifetime of the first excited state. The 0−1 peak, in contrast, contains contributions from both stimulated emission and bleach, so it measures both excited state relaxation and ground state refilling. Given the fact that the decay time constants of the 0−1 and the 1−2 peaks are different, this must imply that vibrational energy first flows very efficiently into some intermediate state (the nature of which we do not know) before it refills the OH ground state, similar to the scheme proposed for example in ref 53. The same effect (albeit with smaller magnitude) has also been observed for the OH-stretch vibration in Ih ice (80 K) with relaxation rates of 0.59 and 0.44 ps for the 0−1 and 1−2 transitions, respectively,[26] as well as in liquid water (363 K) with 1.05 and 0.9 ps, respectively.[53] Furthermore, for the OD-stretch case, the difference of the decay times between the 0−1 and 1−2 transitions becomes smaller as the overall relaxation time increases (Table I), probably since the depopulation of that intermediate state is no longer rate limiting for the longer relaxation times.

To the best of our knowledge, the 240 fs decay time for the OH stretch vibration of HOD/D_2O is the fastest ever observed in any phase of water for that isotope composition; significantly faster than in crystalline ice Ih (440 fs).[26] It is also faster in comparison to the OD stretch vibration of HOD/H_2O, presumably because the OH excitation explores a higher part of the potential and as such experiences more of its anharmonicity. The beating structure in the 1−2 peak decay (Figure 6) indicates that intermolecular hydrogen bond modes strongly couple to the OH vibration and thus might play an important role in the ultrafast decay. Furthermore, although the Fermi resonance between the first overtone of HOD bend and the first excited state of the OH stretch is not nearly as close as that observed for the second excited state of the OH stretch (the HOD fundamental observed at 1490 cm^{-1}, so its overtone is presumably close to 2980 cm^{-1} while the peak of the OH fundamental is at 3280 cm^{-1}), it still might contribute an efficient energy relaxation pathway.[54−56]

In conclusion, we consider the 2D IR spectra of LDA ice higher resolution spectra of water in a form, which is structurally relatively similar to the liquid phase (at least, more similar than to crystalline ice). These spectra allow us to measure the properties of the hydrogen bond potential, such as anharmonicity, relaxation rates, and spectral width of 0−1 and 1−2 transitions, more accurately, because the response is not smeared out by fast spectral diffusion present in liquid water. For the OD vibration of HOD in H_2O, a single mode picture can describe the 2D IR response well, that is, all bands can clearly be assigned as ground, first, or second excited state of

the OD stretch vibration. The diagonal and off-diagonal anharmonicity increases with hydrogen bond strength, and hence also the relaxation rate. In contrast, specific couplings to other modes can be identified for the OH vibration of HOD in D_2O, such as a Fermi resonance with the HOD bend vibration and coupling to phonon modes. The various anharmonic features deduced from these 2D IR spectra provide cornerstones for the development of the hydrogen bond potentials of water.

AUTHOR INFORMATION

Corresponding Author

*E-mail: phamm@pci.uzh.ch.

Notes

The authors declare no competing financial interest.

ACKNOWLEDGMENTS

We thanks Jan Helbing for significant help in the lab. The work has been supported by the Swiss National Science Foundation (SNF) through the National Center of Competence and Research (NCCR) MUST.

REFERENCES

(1) Zheligovskaya, E. A.; Malenkov, G. G. Crystalline water ices. *Russ. Chem. Rev.* **2006**, *75* (1), 57.

(2) Salzmann, C. G.; Radaelli, P. G.; Mayer, E.; Finney, J. L. Ice XV: A new thermodynamically stable phase of ice. *Phys. Rev. Lett.* **2009**, *103* (10), 105701.

(3) Loerting, T.; Giovambattista, N. Amorphous ices: experiments and numerical simulations. *J. Phys.: Cond. Matter* **2006**, *18* (50), R919−R977.

(4) Loerting, T.; Winkel, K.; Seidl, M.; Bauer, M.; Mitterdorfer, C.; Handle, P. H.; Salzmann, C. G.; Mayer, E.; Finney, J. L.; Bowron, D. T. How many amorphous ices are there? *Phys. Chem. Chem. Phys.* **2011**, *13* (19), 8783−8794.

(5) Dubochet, J.; Adrian, M.; Chang, J. J.; Homo, J. C.; Lepault, J.; Mcdowall, A. W.; Schultz, P. Cryo-electron microscopy of vitrified specimens. *Q. Rev. Biophys.* **1988**, *21* (2), 129−228.

(6) Mayer, E.; Pletzer, R. Astrophysical implications of amorphous ice - a microporous solid. *Nature* **1986**, *319* (6051), 298−301.

(7) Debenedetti, P. G. Supercooled and glassy water. *J. Phys.: Condens. Matter* **2003**, *15* (45), R1669−R1726.

(8) Poole, P. H.; Sciortino, F.; Essmann, U.; Stanley, H. E. Phase-behavior of metastable water. *Nature* **1992**, *360* (6402), 324−328.

(9) Mishima, O.; Stanley, H. E. The relationship between liquid, supercooled and glassy water. *Nature* **1998**, *396* (6709), 329−335.

(10) Tulk, C. A.; Benmore, C. J.; Urquidi, J.; Klug, D. D.; Neuefeind, J.; Tomberli, B.; Egelstaff, P. A. Structural studies of several distinct metastable forms of amorphous ice. *Science* **2002**, *297* (5585), 1320−1323.

(11) Guthrie, M.; Urquidi, J.; Tulk, C. A.; Benmore, C. J.; Klug, D. D.; Neuefeind, J. Direct structural measurements of relaxation processes during transformations in amorphous ice. *Phys. Rev. B* **2003**, *68* (18), 184110.

(12) Klotz, S.; Strassle, T.; Nelmes, R. J.; Loveday, J. S.; Hamel, G.; Rousse, G.; Canny, B.; Chervin, J. C.; Saitta, A. M. Nature of the polyamorphic transition in ice under pressure. *Phys. Rev. Lett.* **2005**, *94* (2), 025506.

(13) Kim, C. U.; Barstow, B.; Tate, M. W.; Gruner, S. M. Evidence for liquid water during the high-density to low-density amorphous ice transition. *Proc. Natl. Acad. Sci. USA* **2009**, *106* (12), 4596−4600.

(14) Bergren, M. S.; Schuh, D.; Sceats, M. G.; Rice, S. A. The OH stretching region infrared-spectra of low-density amorphous solid water and polycrystalline ice Ih. *J. Chem. Phys.* **1978**, *69* (8), 3477−3482.

(15) Hagen, W.; Tielens, A. G. G. M.; Greenberg, J. M. The infrared-spectra of amorphous solid water and ice Ic between 10 and 140 K. *Chem. Phys.* **1981**, *56* (3), 367−379.

(16) Sivakumar, T. C.; Schuh, D.; Sceats, M. G.; Rice, S. A. 2500−4000 cm^{-1} Raman and IR-spectra of low-density amorphous solid water and of polycrystalline ice. I. *Chem. Phys. Lett.* **1977**, *48* (2), 212−218.

(17) Klug, D. D.; Mishima, O.; Whalley, E. High-density amorphous ice. IV. Raman-spectrum of the uncoupled O-H and O-D oscillators. *J. Chem. Phys.* **1987**, *86* (10), 5323−5328.

(18) Loerting, T.; Schustereder, W.; Winkel, K.; Salzmann, C. G.; Kohl, I.; Mayer, E. Amorphous ice: Stepwise formation of very-high-density amorphous ice from low-density amorphous ice at 125 K. *Phys. Rev. Lett.* **2006**, *96* (2), 025702.

(19) Nilsson, A.; Pettersson, L. G. M. Perspective on the structure of liquid water. *Chem. Phys.* **2011**, *389* (1−3), 1−34.

(20) Finney, J. L.; Hallbrucker, A.; Kohl, I.; Soper, A. K.; Bowron, D. T. Structures of high and low density amorphous ice by neutron diffraction. *Phys. Rev. Lett.* **2002**, *88* (22), 225503.

(21) Winkel, K.; Bowron, D. T.; Loerting, T.; Mayer, E.; Finney, J. L. Relaxation effects in low density amorphous ice: Two distinct structural states observed by neutron diffraction. *J. Chem. Phys.* **2009**, *130* (20), 204502.

(22) Bellissentfunel, M. C.; Teixeira, J.; Bosio, L. Structure of high-density amorphous water. II. Neutron-scattering study. *J. Chem. Phys.* **1987**, *87* (4), 2231−2235.

(23) Seifert, G.; Weidlich, K.; Graener, H. Picosecond IR hole-burning spectroscopy on HDO ice Ih. *Phys. Rev. B* **1997**, *56* (22), 14231−14234.

(24) Dokter, A. M.; Bakker, H. J. Transient absorption of vibrationally excited ice Ih. *J. Chem. Phys.* **2008**, *128* (2), 024502.

(25) Li, F.; Skinner, J. L. Infrared and raman line shapes for ice Ih. I. Dilute HOD in H_2O and D_2O. *J. Chem. Phys.* **2010**, *132* (20), 204505.

(26) Perakis, F.; Widmer, S.; Hamm, P. Two-dimensional infrared spectroscopy of isotope-diluted ice Ih. *J. Chem. Phys.* **2011**, *134*, 204505.

(27) Perakis, F.; Hamm, P. Two-dimensional infrared spectroscopy of neat ice Ih. *Phys. Chem. Chem. Phys.* **2012**, *14* (18), 6250−6256.

(28) Asbury, J. B.; Steinel, T.; Kwak, K.; Corcelli, S. A.; Lawrence, C. P.; Skinner, J. L.; Fayer, M. D. Dynamics of water probed with vibrational echo correlation spectroscopy. *J. Chem. Phys.* **2004**, *121* (24), 12431−12446.

(29) Eaves, J. D.; Loparo, J. J.; Fecko, C. J.; Roberts, S. T.; Tokmakoff, A.; Geissler, P. L. Hydrogen bonds in liquid water are broken only fleetingly. *Proc. Natl. Acad. Sci. U.S.A.* **2005**, *102*, 13019−13022.

(30) Yeremenko, S.; Pshenichnikov, M. S.; Wiersma, D. A. Hydrogen-bond dynamics in water explored by heterodyne-detected photon echo. *Chem. Phys. Lett.* **2003**, *369*, 107−113.

(31) Cowan, M. L.; Bruner, B. D.; Huse, N.; Dwyer, J. R.; Chugh, B.; Nibbering, E. T. J.; Elsaesser, T.; Miller, R. J. D. Ultrafast memory loss and energy redistribution in the hydrogen bond network of liquid H_2O. *Nature* **2005**, *434*, 199−202.

(32) Perakis, F.; Hamm, P. Two-dimensional infrared spectroscopy of supercooled water. *J. Phys. Chem. B* **2011**, *115*, 5289−5293.

(33) Hamm, P.; Zanni, M. T. *Concepts and Methods of 2D Infrared Spectrsocopy*; Cambridge University Press: Cambridge, 2011.

(34) Gale, G. M.; Gallot, G.; Hache, F.; Lascoux, N.; Bratos, S.; Leicknam, J. C. Femtosecond dynamics of hydrogen bonds in liquid water: A real time study. *Phys. Rev. Lett.* **1999**, *82* (5), 1068−1071.

(35) Steinel, T.; Asbury, J. B.; Corcelli, S. A.; Lawrence, C. P.; Skinner, J. L.; Fayer, M. D. Water dynamics: dependence on local structure probed with vibrational echo correlation spectroscopy. *Chem. Phys. Lett.* **2004**, *386* (4−6), 295−300.

(36) Corcelli, S. A.; Lawrence, C. P.; Skinner, J. L. Combined electronic structure/molecular dynamics approach for ultrafast infrared spectroscopy of dilute HOD in liquid H_2O and D_2O. *J. Chem. Phys.* **2004**, *120* (17), 8107−8117.

(37) Moller, K. B.; Rey, R.; Hynes, J. T. Hydrogen bond dynamics in water and ultrafast infrared spectroscopy: A theoretical study. *J. Phys. Chem. A* **2004**, *108*, 1275−1289.
(38) Smith, J. D.; Cappa, C. D.; Wilson, K. R.; Cohen, R. C.; Geissler, P. L.; Saykally, R. J. Unified description of temperature-dependent hydrogen-bond rearrangements in liquid water. *Proc. Natl. Acad. Sci. U.S.A.* **2005**, *102*, 14171−14174.
(39) Hamm, P.; Kaindl, R. A.; Stenger, J. Noise suppression in femtosecond mid-infrared light sources. *Opt. Lett.* **2000**, *25* (24), 1798−1800.
(40) DeFlores, L.; Nicodemus, R.; Tokmakoff, A. Two dimensonal Fourier transform spectroscopy in the pump-probe geometry. *Opt. Lett.* **2007**, *32* (20), 2966−2968.
(41) Helbing, J.; Hamm, P. Compact implementation of Fourier transform two-dimensional IR spectroscopy without phase ambiguity. *J. Opt. Soc. Am. B* **2011**, *28* (1), 171−178.
(42) Bloem, R.; Garrett-Roe, S.; Strzalka, H.; Hamm, P.; Donaldson, P. Enhancing signal detection and completely eliminating scattering using quasi-phase-cycling in 2D IR experiments. *Opt. Express* **2010**, *18* (26), 27067−27078.
(43) Burton, E. F.; Oliver, W. F. The crystal structure of ice at low temperature. *Proc. R. Soc. Lond. A* **1935**, *153* (878), 166−172.
(44) Beaumont, R. H.; Chihara, H.; Morrison, J. A. Transitions between different forms of ice. *J. Chem. Phys.* **1961**, *34* (4), 1456.
(45) Corcelli, S. A.; Skinner, J. L. Infrared and Raman line shapes of dilute HOD in liquid H_2O and D_2O from 10 to 90 °C. *J. Phys. Chem. A* **2005**, *109* (28), 6154−6165.
(46) Fulmer, E. C.; Ding, F.; Zanni, M. T. Heterodyned fifth-order 2D-IR spectroscopy of the azide ion in an ionic glass. *J. Chem. Phys.* **2005**, *122*, 034302.
(47) Kwak, K.; Rosenfeld, D. E.; Fayer, M. D. Taking apart the two-dimensional infrared vibrational echo spectra: More information and elimination of distortions. *J. Chem. Phys.* **2008**, *128* (20), 204505.
(48) Schmidt, J. R.; Corcelli, S. A.; Skinner, J. L. Pronounced non-Condon effects in the ultrafast infrared spectroscopy of water. *J. Chem. Phys.* **2005**, *123*, 044513.
(49) Fecko, C. J.; Eaves, J. D.; Loparo, J. J.; Tokmakoff, A.; Geissler, P. L. Ultrafast hydrogen-bond dynamics in the infrared spectroscopy of water. *Science* **2003**, *301* (5640), 1698−1702.
(50) Lawrence, C. P.; Skinner, J. L. Vibrational spectroscopy of HOD in liquid D_2O. III. spectral diffusion, and hydrogen-bonding and rotational dynamics. *J. Chem. Phys.* **2003**, *118* (1), 264−272.
(51) Bakker, H. J.; Nienhuys, H. K. Delocalization of protons in liquid water. *Science* **2002**, *297* (5581), 587−590.
(52) Marko, L.; Ramasesha, K.; Tokmakoff, A. Experimental evidence for Fermi resonances in isotropically dilute water from ultrafast broadband IR spectroscopy. *J. Phys. Chem. B.* **2013**, DOI: 10.1021/jp4034613.
(53) Nienhuys, H.-K.; Woutersen, S.; van Santen, R. A.; Bakker, H. J. Mechanism for vibrational relaxation in water investigated by femtosecond infrared spectroscopy. *J. Chem. Phys.* **1999**, *111*, 1494.
(54) Deak, J. C.; Rhea, S. T.; Iwaki, L. K.; Dlott, D. D. Vibrational energy relaxation and spectral diffusion in water and deuterated water. *J. Phys. Chem. A* **2000**, *104* (21), 4866−4875.
(55) Wang, Z. H.; Pakoulev, A.; Pang, Y.; Dlott, D. D. Vibrational substructure in the OH stretching transition of water and HOD. *J. Phys. Chem. A* **2004**, *108* (42), 9054−9063.
(56) Rey, R.; Ingrosso, F.; Elsaesser, T.; Hynes, J. T. Pathways for H_2O bend vibrational relaxation in liquid water. *J. Phys. Chem. A* **2009**, *113* (31), 8949−8962.